

Research Article

Prediction of cytochrome P450-mediated drug clearance in humans based on the measured activities of selected CYPs

Jie Gao¹, Jie Wang¹, Na Gao¹, Xin Tian¹, Jun Zhou¹, Yan Fang¹, Hai-Feng Zhang¹, Qiang Wen¹, Lin-Jing Jia¹, Dan Zou² and Hai-Ling Qiao¹

¹Institute of Clinical Pharmacology, Zhengzhou University, Zhengzhou, China; ²Department of Histology and Embryology, Henan Medical College, Zhengzhou, China

Correspondence: Hai-Ling Qiao (qiaohl@zzu.edu.cn) or Dan Zou (zd6986@sina.com)



Determining drug-metabolizing enzyme activities on an individual basis is an important component of personalized medicine, and cytochrome P450 enzymes (CYPs) play a principal role in hepatic drug metabolism. Herein, a simple method for predicting the major CYP-mediated drug clearance *in vitro* and *in vivo* is presented. Ten CYP-mediated drug metabolic activities in human liver microsomes (HLMs) from 105 normal liver samples were determined. The descriptive models for predicting the activities of these CYPs in HLMs were developed solely on the basis of the measured activities of a smaller number of more readily assayed CYPs. The descriptive models then were combined with the Conventional Bias Corrected *in vitro*–*in vivo* extrapolation method to extrapolate drug clearance *in vivo*. The V_{\max} , K_m , and CL_{int} of six CYPs (CYP2A6, 2C8, 2D6, 2E1, and 3A4/5) could be predicted by measuring the activities of four CYPs (CYP1A2, 2B6, 2C9, and 2C19) in HLMs. Based on the predicted CL_{int} , the values of CYP2A6-, 2C8-, 2D6-, 2E1-, and 3A4/5-mediated drug clearance *in vivo* were extrapolated and found that the values for all five drugs were close to the observed clearance *in vivo*. The percentage of extrapolated values of clearance *in vivo* which fell within 2-fold of the observed clearance ranged from 75.2% to 98.1%. These findings suggest that measuring the activity of CYP1A2, 2B6, 2C9, and 2C19 allowed us to accurately predict CYP2A6-, 2C8-, 2D6-, 2E1-, and 3A4/5-mediated activities *in vitro* and *in vivo* and may possibly be helpful for the assessment of an individual's drug metabolic profile.

Introduction

As the principal class of hepatic drug metabolizing enzymes, CYPs play a critically important role in the biosynthesis and degradation of endogenous compounds and the metabolism of drugs and environmental procarcinogens [1]. Interindividual variation in drug metabolism, which encompasses genetic polymorphisms of CYPs [2,3], smoking [2,3], drinking [2,3], age [4], and gender [5,6], has a substantial impact on individual drug safety and efficacy, raising a challenge to guide individualized medicine.

It is usually agreed that patient differences in pharmacokinetics largely result from differences in the activities of an individual's drug metabolizing enzymes, and is the chief reason for different responses to drugs [7–9]. Therefore, determining the drug metabolizing enzyme activities of an individual is an important prerequisite for personalized medicine. In addition, the area under the blood concentration–time curve and the steady-state blood concentration depend on drug clearance *in vivo* (CL_H) considered to be directly related to the pharmacological effects or adverse effects of a drug. Therefore, having information on the CL_H is a necessary condition for individual dosage regimens.

Received: 16 August 2017
Revised: 14 October 2017
Accepted: 17 October 2017

Accepted Manuscript Online:
20 October 2017
Version of Record published:
21 November 2017

A multitude of different CYPs share similar physical and molecular characteristics, are colocalized on the cytoplasmic side of the endoplasmic reticulum [10,11], and coordinately carry out the biosynthesis and degradation of endogenous steroids, lipids, and vitamins as well as many exogenous substances [12-15]. In addition, a substantial degree of correlation among microsomal CYP activities was reported in two previous studies [4,16]. Another study found that the expression levels of almost all xenobiotic-metabolizing genes were strongly correlated with each other at the mRNA level [17]. Our previous studies also have shown that a high degree of correlation existed at the mRNA and protein expression levels of CYPs [18]. These correlations among CYPs at the protein, mRNA, and activity levels suggest that descriptive models based on multiple linear regression might be developed to predict the activities of some CYPs solely on the basis of measured activities of a smaller number of more readily assayed CYP enzymes.

In vitro–*in vivo* extrapolation (IVIVE) is an important method for estimating the *in vivo* clearance of drugs based on the *in vitro* intrinsic clearance data determined in human liver microsomes [19]. The IVIVE method is useful in providing insight into the rate of elimination of drugs from the body and helping physicians make dosage adjustments. Recently, to predict the *in vivo* clearance for CYPs more accurately, we introduced correction coefficients into the IVIVE method based on the study of Halifax and Houston, who developed the conventional bias corrected *in vitro*–*in vivo* extrapolation (CBC-IVIVE) method [2,20]. Combining descriptive models and CBC-IVIVE might allow us to accurately predict total CYP-mediated drug clearance *in vivo* based on the measured activities of a few CYPs using a small quantity of liver tissue.

Herein, we obtained 105 liver tissue samples derived from 123 liver samples [21] taken from normal tissue adjacent to surgical biopsies, which allowed us to measure the activities of six CYPs in each sample and provided the foundation for the development of descriptive models that could be used to estimate the activities of six CYPs by actually measuring four CYP activities. To strengthen the clinical values, the CL_H of probe drugs for six CYPs were extrapolated using CBC-IVIVE method, and the extrapolation accuracy was evaluated.

Materials and methods

Chemicals and reagents

All probe drugs (phenacetin, coumarin, bupropion, paclitaxel, tolbutamide, omeprazole, dextromethorphan, chlorzoxazone, and midazolam) and one metabolite (acetaminophen) were purchased from the National Institute for the Food and Drug Control (China). Other metabolites (7-OH-coumarin, 4-OH-bupropion, 6-OH-paclitaxel, 4-OH-tolbutamide, 4-OH-omeprazole, 3-methoxymorphinan, 6-OH-chlorzoxazone, and 1-OH-midazolam) were obtained from Toronto Research Chemicals, Inc. (Canada). Reduced nicotinamide adenine dinucleotide phosphate and horse cytochrome C were obtained from Solarbio Science and Technology co. (China). Methanol and acetonitrile were HPLC grade and were purchased from Siyou Chemical Reagent Co. (China).

Human liver microsomes (HLMs)

As reported recently [21], 105 liver samples were selected from 123 liver samples obtained from patients undergoing liver surgery during 2012 and 2014 at the First Affiliated Hospital of Zhengzhou University, the People's Hospital of Henan Province, and the Tumors' Hospital of Henan Province. The present study was conducted according to the World Medical Association Declaration of Helsinki, authorized by the ethics committees of Zhengzhou University (Zhengzhou, China), and written informed consent was obtained from each volunteer. All experiments were performed in accordance with the approved guidelines of the ethics committees of Zhengzhou University.

Detailed information [gender, age, smoking, drinking, body weight (BW), and medical diagnosis] for each patient was well documented. In accord with previous research [22], the smokers were defined as those who smoke 11 or more cigarettes per day and non-smokers were defined as those who smoke less than 11 cigarettes per day or never smoked; drinkers were defined as those who have consumed alcohol 2–3 times or more per week, and non-drinkers were defined as those who have consumed alcohol less than two times per week or never drunk. All patients were subjected to routine anesthetic use for the procedure and had no history of exposure to known CYP-inducing or inhibiting agents. Samples from normal livers were collected, with liver health confirmed by liver function tests, histopathological analysis, and imaging examination by ultrasonography or CT. Following extraction, liver samples were immediately frozen and stored in liquid nitrogen until use. As described recently [23], HLMs were prepared by differential centrifugation and stored at -80°C until analysis. Microsomal protein content was determined by the Bradford method [24].

Measurement of ten CYP-mediated metabolic activities *in vitro*

According to the recent methods [25], ten CYP-mediated metabolic activities were measured in individual assays by incubating HLMs (0.3 mg protein/ml for CYP1A2, 2A6, and 2E1; 0.2 mg protein/ml for CYP2D6 and 3A4/5; 0.5 mg protein/ml for CYP2B6, 2C8, 2C9, and 2C19), 100 mM phosphate buffer (pH 7.4), and 1 mM reduced nicotinamide adenine dinucleotide phosphate with seven or eight concentrations of substrate (6.25–800 μ M for phenacetin, 0.156–20 μ M for coumarin, 7.8–500 μ M for bupropion, 2.5–80 μ M for paclitaxel, 31.25–2000 μ M for tolbutamide, 3.9–500 μ M for omeprazole, 0.625–960 μ M for dextromethorphan, 7.8–1000 μ M for chlorzoxazone, and 0.39–50 μ M for midazolam). The mixtures were preincubated for 5 min at 37°C. Optimal incubation times were as follows: 30 min for phenacetin *O*-deethylation, coumarin 7-hydroxylation, and chlorzoxazone 6-hydroxylation; 60 min for bupropion 4-hydroxylation and tolbutamide 4-hydroxylation; 90 min for omeprazole 5-hydroxylation; 120 min for paclitaxel 6-hydroxylation; 20 min for dextromethorphan *O*-demethylation; and 5 min for midazolam 1'-hydroxylation. Incubation conditions ensured linear metabolite formation with respect to reaction time and protein content.

Reactions were terminated by adding 20 μ l of ice-cold acetonitrile (phenacetin, omeprazole, and midazolam), 1 ml of ethylacetate (paclitaxel and chlorzoxazone), or 10 μ l of perchloric acid (coumarin, bupropion, tolbutamide, and dextromethorphan). Substrate metabolites were identified by HPLC-UV (acetaminophen, 4-OH-bupropion, 6-OH-paclitaxel, 4-OH-tolbutamide, 4-OH-omeprazole, 6-OH-chlorzoxazone, and 1-OH-midazolam) or HPLC-FLD (7-OH-coumarin and 3-methoxymorphinan). The detailed description of analytical methods for the substrate metabolites is provided in Supplementary Table S1. The Michaelis–Menten constant (K_m) and maximum reaction rate (V_{max}) of each CYP were determined by nonlinear regression analysis using GraphPad Prism 5.04 (GraphPad Inc., La Jolla, CA, U.S.A.). Intrinsic clearance (CL_{int}) was calculated based on the ratio of V_{max} -to- K_m .

Prediction of six CYP-mediated metabolic activities *in vitro*

Development of descriptive models

Predictive descriptive models for each kinetic parameter (V_{max} , K_m , and CL_{int}) for each CYP can be developed using SPSS 17.0 (SPSS Inc., Chicago, IL, U.S.A.), as follows: First, each kinetic parameter (V_{max} , K_m , and CL_{int}) of the ten CYPs was treated as a dataset, which then generated three datasets. For each training set, the data of one CYP were set as the dependent variable and the datasets of the other CYPs were set as independent variables, from which a multiple linear regression model was developed by a stepwise method (criteria: probability of F to enter was ≤ 0.05 , probability of F to remove was ≥ 0.10). For every model, the coefficient of determination (R^2) and adjusted coefficient of determination (R^2_{ad}) were calculated.

Prediction of activities for six CYPs

A full-scale analysis of all multiple linear regression equations was determined based on the *ab initio* assumption that CYP activity was independent of other enzyme activities. Using the equations generated and refined above, it was found that the activities of six CYPs (CYP2A6, 2C8, 2D6, 2E, and 3A4/5) could be predicted based on the measured activities of four CYPs (CYP1A2, 2B6, 2C9, and 2C19).

Accuracy of predicted CL_{int}

As only the CL_{int} was used to extrapolate the CL_H , the accuracy of the predicted CL_{int} was evaluated. The normality of the data distribution was first assessed using the method of Kolmogorov–Smirnov and Shapiro–Wilk. Because most datasets were not normally distributed, the overall accuracy of prediction was explored using Mann–Whitney U test to compare the different distribution between the measured and predicted CL_{int} . In order to estimate the accuracy of prediction for each case, the ratio of predicted CL_{int} -to-measured CL_{int} for every individual was calculated and a 2-fold precision limit was set.

Extrapolation of six CYP-mediated drug clearance values *in vivo*

CBC-IVIVE method

According to previous reports [2,20], the equation of the CBC-IVIVE is

$$CL_H = CC \times \frac{Q_H \times CL_{int} \times MPPGL \times (LW/BW \times f_{u,p}/R_B)}{Q_H + CL_{int} \times MPPGL \times (LW/BW \times f_{u,p}/R_B)}$$

Table 1 The basic clinical characteristics of human liver samples (n=105)

Variables	Group	Number (percent)
Gender	Male	37 (35.2%)
	Female	68 (64.8%)
Age (years)	<44	35 (33.3%)
	45–59	56 (53.3%)
	60–74	13 (12.4%)
	>75	1 (1.0%)
Smoking	Yes	12 (11.9%)
	No	89 (88.1%)
Drinking	Yes	12 (11.9%)
	No	89 (88.1%)
Medical diagnosis	Liver hemangioma	84 (80.0%)
	Cholelithiasis	9 (8.6%)
	Metastatic carcinoma	8 (7.6%)
	Gallbladder cancer	4 (3.8%)

Where Q_H (ml/min) was determined as 24.5% [26] of the cardiac output. Cardiac output originated from data for normal Han Chinese females (n=805) and males (n=783) [27]. Microsomal protein per gram of liver (MPPGL) contents were determined using cytochrome P450 oxidoreductase activity as measured in homogenates and microsomes obtained from the same liver tissue sample [28,29]; The liver weight (LW) was calculated by multiplying the liver volume by the liver density, where liver volume (ml) = $12.5 \times BW + 536.4$ [30] and the liver density was 1.001 g/ml [31]. The correction coefficient (CC), the plasma unbound fraction ($f_{u,p}$), and blood-to-plasma concentration ratio (R_B) of each probe drug for six CYPs were obtained from literature [2,32–36].

Extrapolation-based measured or predicted CL_{int}

According to the CL_{int} (measured or predicted above) and other parameters, CYP2A6, 2C8, 2D6, 2E, and 3A4/5-mediated CL_H values were extrapolated (referred to as predicted CL_H and CL'_H) using the CBC-IVIVE strategy.

Accuracy of predicted CL_H and CL'_H

The overall accuracy of the predictions was assessed from the average fold-error (AFE) and the different distribution between CL_H and CL'_H , while the individual accuracy was assessed based on the individual fold-error (IFE). Because most datasets were not normally distributed, the different distribution between CL_H and CL'_H was explored using Mann–Whitney U test. A 2-fold precision limit corresponds to 0.5–2 of AFE or IFE values, where, $AFE = 10^{1/N[\Sigma \log(\text{predicted mean}/\text{observed overall mean})]}$, $IFE = 10^{1/N[\Sigma \log(\text{predicted individual value}/\text{observed overall mean})]}$ [2]. N refers to the number of separate reports in the literature concerning intravenous drug clearance, except for chlorzoxazone.

Statistical analyses

Statistical analysis was performed using SPSS 17.0 software (SPSS Inc., Chicago, IL, U.S.A.), and a P -value < 0.05 was considered to be statistically significant (two-tailed). All graphs were generated using the Adobe Photoshop CC 2014 and GraphPad Prism 5.04 software package (GraphPad Inc., La Jolla, CA, U.S.A.).

Results

Measurement of ten CYP-mediated metabolic activities *in vitro*

As shown in Table 1, the basic clinical characteristics of human liver samples were collected from 105 subjects. Among all subjects, women in a majority of cases, over half the subjects were between 45 and 59 years old. Most subjects had no smoking or drinking history. Most of the subjects experienced liver hemangioma. All subjects received only regular anesthetics and had no history of exposure to known CYP-inducing or -inhibiting agents.

The above normal Chinese liver samples were used to measure the ten CYPs (CYP1A2, 2A6, 2B6, 2C8, 2C9, 2C19, 2D6, 2E1, and 3A4/5)-mediated metabolic activities *in vitro* using probe substrate metabolism assays. The activities were described as kinetic parameters (V_{max} , K_m , and CL_{int}), and the results are presented in Table 2.

Table 2 The V_{\max} , K_m , and CL_{int} of ten CYPs in human liver microsomes (n=105)

CYPs	V_{\max} (pmol/min/mg protein)	K_m (μM)	CL_{int} ($\mu\text{l}/\text{min}/\text{mg}$ protein)
1A2	754.9(94.9–3154.0)	54.7(4.7–181.6)	14.5(2.8–67.2)
2A6	354.4(3.7–3295.0)	2.3(0.8–10.0)	145.0(1.2–544.7)
2B6	53.3(12.8–333.5)	73.4(17.1–393.3)	0.77(0.13–5.22)
2C8	37.5(2.8–174.6)	14.3(7.0–38.9)	2.70(0.09–6.19)
2C9	256.2(83.8–454.8)	219.2(101.2–555.3)	1.17(0.17–4.18)
2C19	103.9(2.3–381.4)	59.7(20.6–198.3)	1.91(0.01–7.46)
2D6	113.3(23.5–1041.0)	28.9(6.5–260.6)	3.5(0.2–39.5)
2E1	532.1(163.1–1982.0)	52.5(27.1–177.2)	10.5(1.9–39.0)
3A4/5	788.0(69.4–5035.0)	1.9(0.4–10.2)	464.6(8.3–1673.5)

The K_m and V_{\max} of each CYP were determined by nonlinear regression analysis using GraphPad Prism 5.04. The CL_{int} was calculated based on the ratio of V_{\max} to K_m . Data are shown as median and range.

Table 3 The descriptive models for six CYPs in human liver microsomes

Parameters	Regression equation	Known	F	P	R^2	R^2_{ad}
V_{\max} (pmol/min/mg protein)	$2A6 = 104.899 + 2.292 \times 2C19$	2C19	21.559	1.015E–05	0.173	0.165
	$2D6 = 10.698 + 0.481 \times 2C9$	2C9	12.655	5.677E–04	0.109	0.101
	$2E1 = 362.868 + 0.290 \times 1A2$	1A2	25.152	2.217E–06	0.196	0.188
	$2C8 = -6.784 + 0.158 \times 2C9 + 0.143 \times 2B6$	2C9, 2B6	24.813	1.656E–09	0.327	0.314
	$3A4/5 = 106.151 + 9.416 \times 2B6 + 2.504 \times 2C19$	2B6, 2C19	21.209	1.985E–08	0.294	0.280
K_m (μM)	$3A4/5 = 2.941 - 0.013 \times 1A2$	1A2	7.641	6.762E–03	0.069	0.060
CL_{int} ($\mu\text{l}/\text{min}/\text{mg}$ protein)	$2A6 = 120.384 + 9.662 \times 2C19$	2C19	4.381	3.881E–02	0.041	0.031
	$2C8 = 1.693 + 0.862 \times 2C9$	2C9	31.661	1.590E–07	0.235	0.228
	$2D6 = 3.325 + 1.438 \times 2B6$	2B6	5.250	2.399E–02	0.048	0.039
	$2E1 = 6.414 + 1.218 \times 2C19 + 0.143 \times 1A2$	2C19, 1A2	11.108	4.319E–05	0.179	0.163
	$3A4/5 = 407.070 + 77.635 \times 2C19 - 8.003 \times 1A2 + 87.331 \times 2B6$	2C19, 1A2, 2B6	7.257	1.858E–04	0.177	0.153

R^2 , coefficient of determination; R^2_{ad} , adjusted coefficient of determination.

Prediction of six CYP-mediated metabolic activities *in vitro*

Development of the descriptive models

The descriptive models were developed using a multiple linear regression method, based on measured values. The results show that the descriptive models of V_{\max} and CL_{int} of all ten CYPs and K_m of six CYPs (CYP1A2, 2B6, 2C9, 2C19, and 3A4/5) could be developed, and the essential structures of these models consisted of the measured V_{\max} , CL_{int} , and K_m of CYPs (data not shown). In order to predict activities of several CYPs based on known CYP activities, the principle that the numbers of CYPs were known as little as possible was upheld to analyze all multiple linear regression equations carefully. The results indicate that the six CYPs (CYP2A6, 2C8, 2D6, 2E1, and 3A4/5)-mediated metabolic activities *in vitro* could be predicted if the activities of four CYPs (CYP1A2, 2B6, 2C9, and 2C19) measured *in vitro* were known. Table 3 summarizes the regression equations and statistical parameters of these models.

Table 4 The predicted V_{\max} (pmol/min/mg protein), K_m (μM), and CL_{int} ($\mu\text{l}/\text{min}/\text{mg}$ protein) for six CYPs in human liver microsomes (n=105)

CYPs	Parameter	Median	Range	95%PI
2A6	V_{\max}	344.4	110.3–979.1	154.5–857.4
	K_m	2.5	0.9–5.4	1.3–5.1
	CL_{int}	138.9	120.5–192.5	122.9–176.7
2C8	V_{\max}	42.3	8.4–84.0	12.7–76.9
	K_m	15.0	4.5–30.3	6.8–23.9
	CL_{int}	2.7	1.8–5.3	1.9–4.4
2D6	V_{\max}	133.9	51.0–229.5	52.7–216.5
	K_m	29.6	10.0–49.0	11.3–46.4
	CL_{int}	4.4	3.5–10.8	3.6–8.0
2E1	V_{\max}	581.8	390.3–1227.5	421.8–1115.5
	K_m	53.9	30.8–93.2	36.4–71.9
	CL_{int}	11.0	7.2–18.7	7.9–17.3
3A4/5	V_{\max}	897.7	302.7–3493.1	434.3–1837.2
	K_m	1.8	0.7–4.6	1.0–4.3
	CL_{int}	507.5	235.9–958.3	278.6–871.5

95%PI, 95% prediction interval. The values of V_{\max} and CL_{int} for six CYPs were predicted using the descriptive models summarized in Table 1. Because descriptive models of K_m for most CYPs could not be developed, K_m values of six CYPs were calculated as their respective V_{\max} divided by corresponding CL_{int} .

Prediction of activities for six CYPs

Of note, prediction of some CYP-mediated metabolic activities *in vitro* did not require knowledge of all four CYPs activities; some activities could be predicted on just one or two known CYP activities. More specifically, the V_{\max} of CYP2A6 could be predicted based on the V_{\max} of CYP2C19, the V_{\max} of CYP2D6 could be predicted by the V_{\max} of CYP2C9, the V_{\max} of CYP2E1 could be predicted by the V_{\max} of CYP1A2, the V_{\max} of CYP2C8 could be predicted based on the V_{\max} values of CYP2C9 and 2B6, and the V_{\max} values of CYP3A4/5 could be predicted based on the V_{\max} values of CYP2B6 and 2C19. For CL_{int} , CYP2A6 could be predicted based on CYP2C19, CYP2C8 could be predicted based on CYP2C9, CYP2D6 could be predicted based on CYP2B6, CYP2E1 could be predicted based on CYP1A2 and 2C19, CYP3A4/5 could be predicted based on CYP1A2, 2B6, and 2C19. For K_m , although some descriptive models of CYPs could not be developed, the K_m values of most CYPs could be calculated as their respective V_{\max} divided by corresponding CL_{int} .

Taken together, the activity of CYP2A6 could be predicted based on the activity of CYP2C19, CYP2C8 and 2D6 could be predicted based on CYP2B6 and 2C9, CYP2E1 could be predicted based on CYP2C19 and 1A2, CYP3A4/5 could be predicted based on CYP1A2, 2B6, and 2C19. In short, the prediction for six CYPs needed 1–3 measured CYP values. The median values, ranges, and 95% prediction intervals of predicted V_{\max} , K_m , and CL_{int} for CYP2A6, 2C8, 2D6, 2E1, and 3A4/5 are summarized in Table 4. The biggest individual variations in predicted CL_{int} took place in the CYP3A4/5, reaching to 4.1-fold, followed by that of CYP2D6, CYP2C8, CYP2E1, and CYP2A6, demonstrating the fold-change of 3.1, 2.9, 2.6, and 1.6 respectively.

Accuracy of predicted CL_{int}

Because only the CL_{int} was used to extrapolate the clearance *in vivo*, the accuracy of predicted CL_{int} was estimated. For the overall accuracy of prediction, there were no apparent statistical differences in the measured and predicted CL_{int} values of CYP2A6, 2C8, and 2E1 (Figure 1). Nevertheless, the predicted CL_{int} values of CYP2D6 ($P=0.003$) and 3A4/5 ($P=0.014$) were significantly higher than the measured values. The ranges of predicted CL_{int} for all CYPs were smaller than the measured data. In other words, the predicted CL_{int} values narrowed the interindividual variation of measured values, which might influence the accuracy of the predicted clearance *in vivo*.

To estimate the accuracy of predicted CL_{int} for each case, the ratio of predicted CL_{int} -to-measured CL_{int} for every individual was calculated, and results were presented in Table 5. For most subjects (87.6 percent), the predicted CL_{int} for coumarin and paclitaxel was very close to the measured CL_{int} . However, for nearly half the subjects (47.6 percent) the predicted CL_{int} of dextromethorphan was close to the measured CL_{int} .

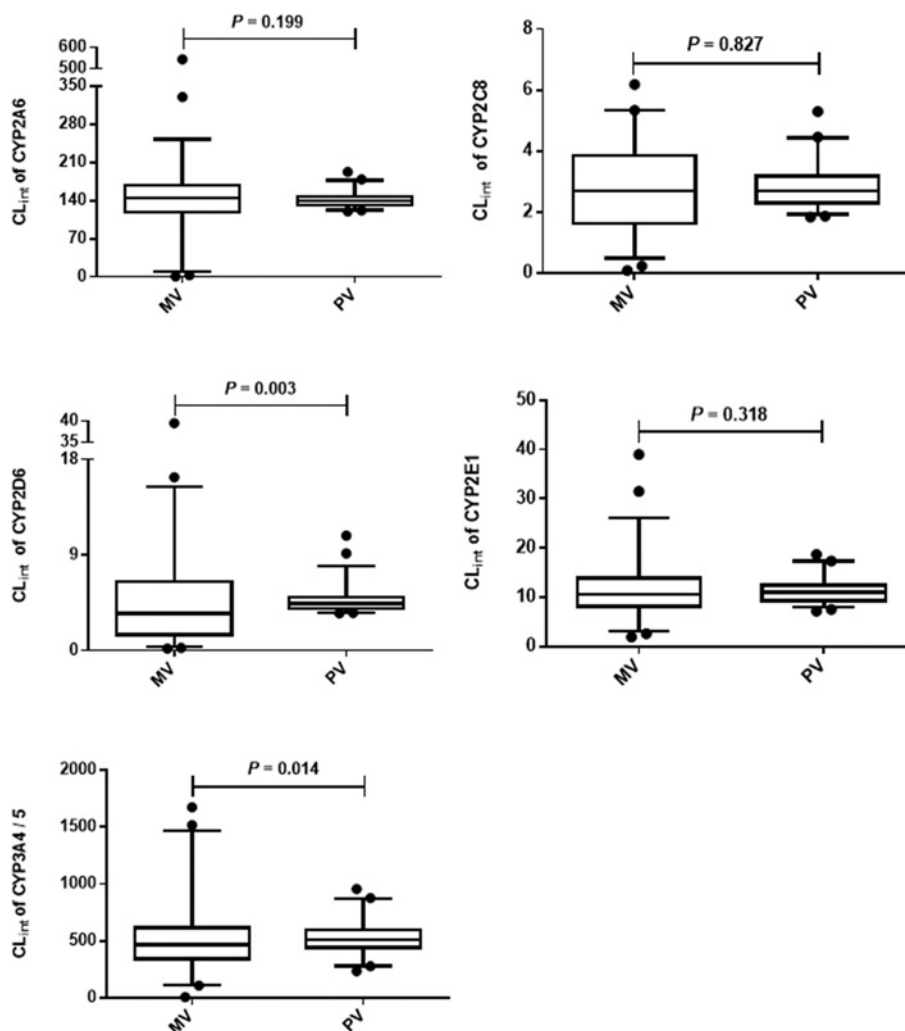


Figure 1. The overall accuracy of predicted CL_{int} of CYP2A6, 2C8, 2D6, 2E1, and 3A4/5

The data are presented as the 2.5–97.5 percentile; Abbreviations: MV, measured value; PV, predicted value determined by the descriptive model. Mann–Whitney U was used to evaluate the difference between predicted and measured values

Table 5 The individual accuracy of predicted CL_{int} (the ratio of predicted CL_{int} -to-measured CL_{int}) of CYP2A6, 2C8, 2D6, 2E1, and 3A4/5 ($n=105$)

CYP	Probe drug	Median	Range	Within a 2-fold error ($n, \%$)
2A6	Coumarin	0.97	0.26–114.7	92 (87.6%)
2C8	Paclitaxel	1.02	0.30–36.3	92 (87.6%)
2D6	Dextromethorphan	1.36	0.13–27.4	50 (47.6%)
2E1	Chlorzoxazone	1.06	0.42–4.96	90 (85.7%)
3A4/5	Midazolam	1.17	0.35–33.7	87 (82.9%)

Extrapolation of six CYP-mediated drug clearance values *in vivo* CBC-IVIVE

The parameters for the equations of the CBC-IVIVE for five probe drugs are based on previous reports and listed in Table 6. Of note, the Q_H , MPPGL, LW, and BW were 1259.3 (1205.4–1629.3) ml/min, 39.6 (9.9–127.9) mg/g, 1337.2 (912.3–1688.1) g, and 64.0 (30.0–92.0) kg respectively. The variable degrees of the other three parameters were relatively lower, with only BW variations reaching 3-fold.

Table 6 The parameters in the equations of the CBC-IVIVE and clearance *in vivo* (CL_H, ml/min) of five probe drugs

CYP	Probe drug	Parameters in the Equation of the CBC-IVIVE*			Observed CL _H	Predicted CL _H (n=105)	Predicted CL' _H (n=105)
		CC	f _{u,p}	R _B			
2A6	Coumarin	5.369 [2]	0.055 [2]	1 [2]	1602.5 ± 547.9 [37]	1602.5 ± 748.2	1692.3 ± 622.8
2C8	Paclitaxel	18.938 [2]	0.098 [32]	0.69 [33]	496.4 ± 210.5 [38-43]	422.2 ± 328.6	413.6 ± 226.8
2D6	Dextromethorphan	35.791 [2]	0.500 [34,35]	0.55 [34,35]	6471.7 ± 5596.7 [44]	6471.7 ± 5816.5	7016.1 ± 3202.7
2E1	Chlorzoxazone	4.152 [2]	0.028 [34]	0.55 [34]	131.4 ± 40.1 [45-49]	131.4 ± 97.4	130.1 ± 69.3
3A4/5	Midazolam	0.540 [2]	0.042 [34,36]	0.54 [34,36]	426.7 ± 95.4 [36,50,51]	403.8 ± 128.3	426.2 ± 95.1

*The equation of the CBC-IVIVE (conventional bias-corrected *in vitro*-*in vivo* extrapolation) was $CL_H = CC \times \frac{Q_H \times CL_{int} \times MPPGL \times (LW/BW \times f_{u,p}/R_B)}{Q_H + CL_{int} \times MPPGL \times (LW/BW \times f_{u,p}/R_B)}$. Abbreviations: BW, body weight; CC, correction coefficient; CL_{int}, intrinsic clearance; LW, liver weight; MPPGL, microsomal protein per gram of liver; Q_H, hepatic blood flow. Observed CL_H was the clearance *in vivo* reported in the literature. Using the CBC-IVIVE method, predicted CL_H was calculated based on measured CL_{int}, and predicted CL'_H was calculated based on predicted CL_{int}.

Extrapolation based on measured CL_{int}

According to the measured CL_{int} in HLMs, the values of CL_H for coumarin, paclitaxel, dextromethorphan, chlorzoxazone, and midazolam which were probe substrates for CYP2A6, 2C8, 2D6, 2E1, and 3A4/5 were extrapolated using the CBC-IVIVE strategy. The predicted and observed CL_H for all five drugs are shown in Table 6. The mean values for the predicted and observed CL_H of coumarin, dextromethorphan, and chlorzoxazone were the same, but the predicted CL_H showed larger individual variations. The mean values for the predicted CL_H of paclitaxel and midazolam were relatively smaller than observed CL_H, but the predicted values showed obvious variations. The individual variation in the values of CL_H for dextromethorphan was the largest, with the coefficient of variation (CV) of 89.9%, followed by that of paclitaxel, chlorzoxazone, and coumarin, demonstrating the CV of 77.8%, 74.1%, and 46.7 respectively. Compared with other drugs, CV of midazolam CL_H was much lower but still achieving 31.8%.

Extrapolation based on predicted CL_{int}

According to the CL_{int} that was predicted above and other parameters, the values of CL'_H for coumarin, paclitaxel, dextromethorphan, chlorzoxazone, and midazolam were extrapolated using the CBC-IVIVE strategy. As shown in Table 6, considering the values of CL'_H for all five drugs, the mean value and SD of CL'_H for midazolam matched best with its observed CL_H, while the mean value CL'_H for dextromethorphan matched poorly with its observed CL_H. The individual variation in the values of CL'_H for paclitaxel was the largest, with the CV of 54.8%, followed by that of chlorzoxazone, dextromethorphan, coumarin, and midazolam, demonstrating the CV of 53.3%, 45.6%, 36.8%, and 22.3% respectively. Compared with the individual variations in the values of CL_H for all five drugs, the individual variations in the values of CL'_H were much smaller.

Accuracy of predicted CL_H and CL'_H

To evaluate the extrapolation performance, the accuracy of the predicted CL_H and CL'_H values for drugs were compared with the observed CL_H (Figure 2). Whether predicted CL_H or CL'_H, the average fold-error (AFE) values for five drugs were adjacent to 1, which demonstrated that the extrapolation performance was accurate. Of note, the values of the predicted CL'_H based on predicted CL_{int} for all five drugs were closer to the observed CL_H than the predicted CL_H based on measured CL_{int}. The predicted CL_H value reduces the difference between individuals, resulting that a more accurate estimate of CL_H than measured CL_{int}.

From another angle to analyze this problem, the distribution of the individual fold-error (IFE) of predicted CL_H and CL'_H for all five drugs were explored (Figure 2). The results support the distributions of IFE for coumarin, paclitaxel, chlorzoxazone, and midazolam in the CL_H and CL'_H groups and showed no significant differences, while there was enough evidence to say that the distributions of IFE for dextromethorphan in the CL_H and CL'_H groups were significantly different.

To test the accuracy of predicted CL_H and CL'_H for each individuals, the IFE was also calculated. The predicted CL'_H value for midazolam matched most closely with its observed CL_H, for which 103 (98.1%) of the cases were within a 2-fold error range (Figure 2). After midazolam, the CL'_H value for coumarin, also matched best with its clearance

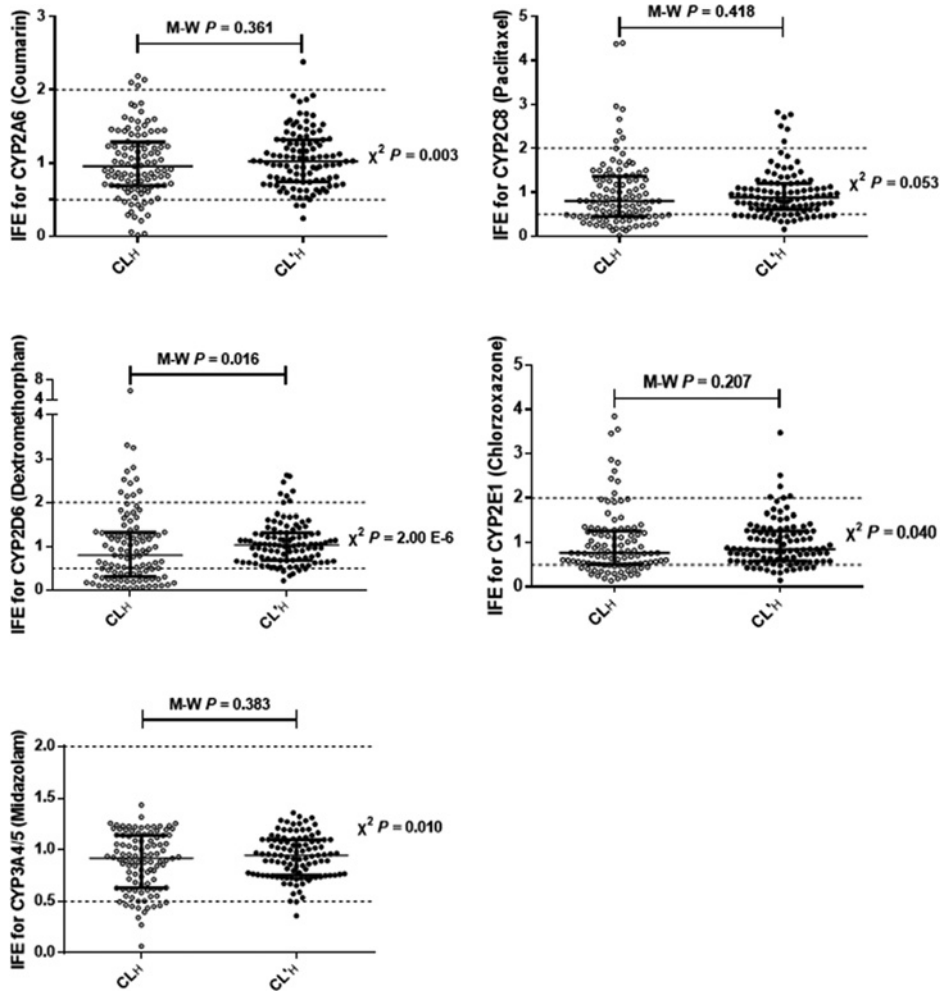


Figure 2. The accuracy of predicted CL_H or CL'_H for coumarin, paclitaxel, dextromethorphan, chlorzoxazone, and midazolam which are the probe substrates of CYP2A6, 2C8, 2D6, 2E1, and 3A4/5 respectively ($n=105$)

IFE is the individual fold-error. CL_H is the *in vivo* clearance or hepatic clearance. Using the conventional bias-corrected *in vitro*–*in vivo* extrapolation method, predicted CL_H was calculated based on measured CL_{int} , and predicted CL'_H was calculated based on predicted CL_{int} . The black horizontal solid line represents the median value and interquartile range. $IFE = 10^{1/N[\sum \log(\text{predicted individual value}/\text{observed overall mean})]}$. Mann–Whitney *U* test was used to evaluate the differences between the IVE of CL_H and CL'_H . Cross tabs with χ^2 tests for independence analyses revealed that the difference between the number (percentage) was within 2-fold error of the observed CL_H in the CL_H and CL'_H groups.

in vivo, for which 101 (96.2%) of the cases were within a 2-fold error range. Meanwhile, the accuracy of predicted CL'_H of dextromethorphan, chlorzoxazone, and paclitaxel for each individuals was also quite outstanding, for which 90 (85.7%), 85 (81.0%), and 79 (75.2%) of the cases respectively, were within a 2-fold error range. While among the five drugs, the predicted CL_H value for midazolam matched most closely with its observed CL_H , for which 93 (88.6%) of the cases were within a 2-fold error range. The number (percent) of predicted CL_H for coumarin, chlorzoxazone, paclitaxel, and dextromethorphan that fell within 2-fold of the observed CL_H were 87 (82.9%), 71 (67.6%), 65 (61.9%), and 58 (55.2%) respectively.

For all five drugs the percentage of predictions that fell within 2-fold of the observed CL_H were different, which used different sources of CL_{int} (measured or predicted). Cross tabs with χ^2 tests for independence analyses revealed that the values of predicted CL'_H for coumarin, dextromethorphan, chlorzoxazone, and midazolam were more accurate than those of predicted CL_H , while the prediction accuracy for paclitaxel was not significantly different between the predicted CL_H and CL'_H using different sources of CL_{int} .

Discussion

The purpose of the present study was to determine the drug clearance values for six CYPs *in vivo* and *in vivo* based on measured activities of four CYPs in HLMs. Descriptive models for predicting the activities of CYPs in HLMs were developed first and the activities of six CYPs (CYP2A6, 2C8, 2D6, 2E1, and 3A4/5) could be predicted by actually measuring the activities of four CYPs (CYP1A2, 2B6, 2C9, and 2C19). In addition, based on the predicted CL_{int} , the clearances for CYP2A6, 2C8, 2D6, 2E1, and 3A4/5 *in vivo* were extrapolated using the CBC-IVIVE method [2,20]. We found that the extrapolation performance was accurate with the AFE values of 1.06, 0.98, 1.08, 0.99, and 0.93 while the number (percent) of predicted CL_H that fell within 2-fold of the observed CL_H were 101 (96.2%), 79 (75.2%), 90 (85.7%), 85 (81.0%), and 103 (98.1%) for coumarin, paclitaxel, dextromethorphan, chlorzoxazone, and midazolam respectively.

Published correlations between different CYP gene and protein expression values could support the models for c_{max} in the present study [17], because the turnover rate is affected by the number of enzyme binding sites, which is determined by protein expression levels. K_m , on the other hand, is about the affinity between substrates and binding sites, which is determined by enzyme and substrate structures. There is no published correlation between structures of CYPs from different chromosomes, although haplotypes exist for some CYPs on the same chromosome. As a consequence of this, predictive models for K_m of some CYPs could not be developed.

Although most previous studies have focused on *in vitro*–*in vivo* extrapolation of metabolic clearance in humans from hepatocyte or HLMs data [19,23,52,53], to our best knowledge, the present study is the first to try to establish descriptive models using a multiple linear regression method and attempt to combine the descriptive models and the CBC-IVIVE to extrapolate drug clearance *in vivo*. Encouragingly, we found that the predicted CL_H values matched most closely with their clearance *in vivo*. To further validate the method established in the present study and the predicted results, the values of predicted CL_H for all five drugs were extrapolated based on measured CL_{int} , which was used for comparative purposes. The results show that the values of predicted CL_H were closer to the observed ones than those of predicted CL_H . In addition, the percentage of predicted CL_H that fell within 2-fold of the observed CL_H for all five drugs were greater than that of the predicted CL_H .

Although these descriptive models could use data on some CYPs to predict activities of others, there are limitations. For example, different probe substrates could result in different observations in CYP3A4 activities due to different substrate binding sites [54]. In the present work, a single substrate was used to reflect the activity of each CYP. Therefore, the models might be applied only to the prediction of activities of substrates which were similar to probe substrates used in the present study. Another limitation is the representativeness of the sample. Although the models were established using the data on ten CYPs from 105 normal liver tissue samples from a Chinese Han population, the models should be further improved and validated in larger samples and in different ethnic groups.

In summary, we developed descriptive models to predict the activities of six CYPs (CYP2A6, 2C8, 2D6, 2E1, and 3A4/5) in HLMs by actually measuring the activities of four CYPs (CYP1A2, 2B6, 2C9, and 2C19). To be helpful for drug development, we combined the descriptive models and the CBC-IVIVE further to extrapolate the CL_H of probe drugs for six CYPs. While this approach has some limitations, it does establish a feasible method that can then be evaluated by additional experimental approaches and in additional populations. These findings may be of benefit for the development of personalized medicine and should be of significant value for drug development.

Funding

This work was supported by the National Natural Science Foundation of China [grant numbers 81473279 and 81673507 (to H.-L.Q.)].

Competing Interests

The authors declare that there are no competing interests associated with the manuscript.

Author Contribution

H.-L.Q. and D.Z. designed the experiments. H.-L.Q., J.G., and D.Z. wrote the manuscript and performed the data analysis. J.G., J.W., N.G., X.T., Y.F., and J.Z. performed the experiments. J.G., H.-F.Z., Y.F., Q.W., and L.-J.J. prepared the human liver microsomes and sample analyzing.

Abbreviations

AFE, average fold-error; BW, body weight; CC, correction coefficient; CBC-IVIVE, conventional bias corrected *in vitro*–*in vivo* extrapolation; CYP, cytochrome P450 enzyme; CL_H , clearance *in vivo*; CL_{int} , intrinsic clearance; CV, coefficient of variation;

$f_{u,p}$, plasma unbound fraction; HLM, human liver microsome; IVIVE, *in vitro*–*in vivo* extrapolation; IFE, individual fold-error; K_m , Michaelis–Menten constant; LW, liver weight; MPPGL, microsomal protein per gram of liver; R_B , blood-to-plasma concentration ratio; R^2 , coefficient of determination; R^2_{ad} , adjusted coefficient of determination; Q_H , cardiac output; V_{max} , maximum reaction rate.

References

- 1 Wilkinson, G.R. (2005) Drug metabolism and variability among patients in drug response. *N. Engl. J. Med.* **352**, 2211–2221, doi:10.1056/NEJMra032424
- 2 Gao, J., Zhou, J., He, X.P., Zhang, Y.F., Gao, N., Tian, X. et al. (2016) Changes in cytochrome P450s-mediated drug clearance in patients with hepatocellular carcinoma *in vitro* and *in vivo*: a bottom-up approach. *Oncotarget* **7**, 28612–28623, doi:10.18632/oncotarget.8704
- 3 Zhou, J., Wen, Q., Li, S.F., Zhang, Y.F., Gao, N., Tian, X. et al. (2016) Significant change of cytochrome P450s activities in patients with hepatocellular carcinoma. *Oncotarget* **7**, 50612–50623, doi:10.18632/oncotarget.9437
- 4 Yang, X., Zhang, B., Molony, C., Chudin, E., Hao, K., Zhu, J. et al. (2010) Systematic genetic and genomic analysis of cytochrome P450 enzyme activities in human liver. *Genome Res.* **20**, 1020–1036, doi:10.1101/gr.103341.109
- 5 Li, J., Wan, Y., Na, S., Liu, X., Dong, G., Yang, Z. et al. (2015) Sex-dependent regulation of hepatic CYP3A by growth hormone: roles of HNF6, C/EBPalpha, and RXRalpha. *Biochem. Pharmacol.* **93**, 92–103, doi:10.1016/j.bcp.2014.10.010
- 6 Wolbold, R., Klein, K., Burk, O., Nussler, A.K., Neuhaus, P., Eichelbaum, M. et al. (2003) Sex is a major determinant of CYP3A4 expression in human liver. *Hepatology* **38**, 978–988, doi:10.1053/jhep.2003.50393
- 7 Ingelman-Sundberg, M. (2004) Pharmacogenetics of cytochrome P450 and its applications in drug therapy: the past, present and future. *Trends Pharmacol. Sci.* **25**, 193–200, doi:10.1016/j.tips.2004.02.007
- 8 Borges, S., Desta, Z., Li, L., Skaar, T.C., Ward, B.A., Nguyen, A. et al. (2006) Quantitative effect of CYP2D6 genotype and inhibitors on tamoxifen metabolism: implication for optimization of breast cancer treatment. *Clin. Pharmacol. Ther.* **80**, 61–74, doi:10.1016/j.cpt.2006.03.013
- 9 Takayama, K., Morisaki, Y., Kuno, S., Nagamoto, Y., Harada, K., Furukawa, N. et al. (2014) Prediction of interindividual differences in hepatic functions and drug sensitivity by using human iPSC-derived hepatocytes. *Proc. Natl. Acad. Sci. U.S.A.* **111**, 16772–16777, doi:10.1073/pnas.1413481111
- 10 Davydov, D.R., Davydova, N.Y., Sineva, E.V. and Halpert, J.R. (2015) Interactions among cytochromes P450 in microsomal membranes: oligomerization of cytochromes P450 3A4, 3A5, and 2E1 and its functional consequences. *J. Biol. Chem.* **290**, 3850–3864, doi:10.1074/jbc.M114.615443
- 11 Reed, J.R. and Backes, W.L. (2012) Formation of P450. P450 complexes and their effect on P450 function. *Pharmacol. Ther.* **133**, 299–310, doi:10.1016/j.pharmthera.2011.11.009
- 12 Nelson, D.R., Koymans, L., Kamataki, T., Stegeman, J.J., Feyereisen, R., Waxman, D.J. et al. (1996) P450 superfamily: update on new sequences, gene mapping, accession numbers and nomenclature. *Pharmacogenetics* **6**, 1–42
- 13 Aguiar, M., Masse, R. and Gibbs, B.F. (2005) Regulation of cytochrome P450 by posttranslational modification. *Drug Metab. Rev.* **37**, 379–404, doi:10.1081/DMR-46136
- 14 Plant, N. (2007) The human cytochrome P450 sub-family: transcriptional regulation, inter-individual variation and interaction networks. *Biochim. Biophys. Acta* **1770**, 478–488, doi:10.1016/j.bbagen.2006.09.024
- 15 Nebert, D.W. and Russell, D.W. (2002) Clinical importance of the cytochromes P450. *Lancet North Am. Ed.* **360**, 1155–1162, doi:10.1016/s0140-6736(02)11203-7
- 16 Wortham, M., Czerwinski, M., He, L., Parkinson, A. and Wan, Y.J. (2007) Expression of constitutive androstane receptor, hepatic nuclear factor 4 alpha, and P450 oxidoreductase genes determines interindividual variability in basal expression and activity of a broad scope of xenobiotic metabolism genes in the human liver. *Drug Metab. Dispos.* **35**, 1700–1710, doi:10.1124/dmd.107.016436
- 17 Wang, D., Jiang, Z., Shen, Z., Wang, H., Wang, B., Shou, W. et al. (2011) Functional evaluation of genetic and environmental regulators of p450 mRNA levels. *PLoS One* **6**, e24900, doi:10.1371/journal.pone.0024900
- 18 Zhang, H.F., Wang, H.H., Gao, N., Wei, J., Tian, X., Zhao, Y. et al. (2016) Physiological content and intrinsic activities of 10 cytochrome P450 isoforms in human normal liver microsomes. *J. Pharmacol. Exp. Ther.*, doi:10.1124/jpet.116.233635
- 19 Poulin, P., Hop, C.E., Ho, Q., Halladay, J.S., Haddad, S. and Kenny, J.R. (2012) Comparative assessment of *In Vitro*–*In Vivo* extrapolation methods used for predicting hepatic metabolic clearance of drugs. *J. Pharm. Sci.* **101**, 4308–4326, doi:10.1002/jps.23288
- 20 Hallifax, D. and Houston, J.B. (2012) Evaluation of hepatic clearance prediction using *in vitro* data: emphasis on fraction unbound in plasma and drug ionisation using a database of 107 drugs. *J. Pharm. Sci.* **101**, 2645–2652, doi:10.1002/jps.23202
- 21 Zhang, H., Gao, N., Liu, T., Fang, Y., Qi, B., Wen, Q. et al. (2015) Effect of cytochrome b5 content on the activity of polymorphic CYP1A2, 2B6, and 2E1 in human liver microsomes. *PLoS One* **10**, e0128547, doi:10.1371/journal.pone.0128547
- 22 Gao, N., Qi, B., Liu, F.J., Fang, Y., Zhou, J., Jia, L.J. et al. (2014) Inhibition of baicalin on metabolism of phenacetin, a probe of CYP1A2, in human liver microsomes and in rats. *PLoS One* **9**, e89752, doi:10.1371/journal.pone.0089752
- 23 Zhang, H., Gao, N., Tian, X., Liu, T., Fang, Y., Zhou, J. et al. (2015) Content and activity of human liver microsomal protein and prediction of individual hepatic clearance *in vivo*. *Sci. Rep.* **5**, 17671, doi:10.1038/srep17671
- 24 Bradford, M.M. (1976) A rapid and sensitive method for the quantitation of microgram quantities of protein utilizing the principle of protein-dye binding. *Anal. Biochem.* **72**, 248–254
- 25 Gao, N., Tian, X., Fang, Y., Zhou, J., Zhang, H., Wen, Q. et al. (2016) Gene polymorphisms and contents of cytochrome P450s have only limited effects on metabolic activities in human liver microsomes. *Eur. J. Pharm. Sci.* **92**, 86–97, doi:10.1016/j.ejps.2016.06.015

- 26 Barter, Z.E., Tucker, G.T. and Rowland-Yeo, K. (2013) Differences in cytochrome p450-mediated pharmacokinetics between chinese and caucasian populations predicted by mechanistic physiologically based pharmacokinetic modelling. *Clin. Pharmacokinet.* **52**, 1085–1100, doi:10.1007/s40262-013-0089-y
- 27 Li, G.F., Yu, G., Liu, H.X. and Zheng, Q.S. (2014) Ethnic-specific in vitro-in vivo extrapolation and physiologically based pharmacokinetic approaches to predict cytochrome P450-mediated pharmacokinetics in the Chinese population: opportunities and challenges. *Clin. Pharmacokinet.* **53**, 197–202, doi:10.1007/s40262-013-0119-9
- 28 Wilson, Z.E., Rostami-Hodjegan, A., Burn, J.L., Tooley, A., Boyle, J., Ellis, S.W. et al. (2003) Inter-individual variability in levels of human microsomal protein and hepatocellularity per gram of liver. *Br. J. Clin. Pharmacol.* **56**, 433–440
- 29 De Bock, L., Boussey, K., De Bruyne, R., Van Winckel, M., Stephenne, X., Sokal, E. et al. (2014) Microsomal protein per gram of liver (MPPGL) in paediatric biliary atresia patients. *Biopharm. Drug Dispos.* **35**, 308–312, doi:10.1002/bdd.1895
- 30 Wang, X.F., Li, B., Lan, X., Yuan, D., Zhang, M., Wei, Y.G. et al. (2008) Establishment of formula predicting adult standard liver volume for liver transplantation. *Zhonghua Wai Ke Za Zhi* **46**, 1129–1132
- 31 Yuan, D., Lu, T., Wei, Y.G., Li, B., Yan, L.N., Zeng, Y. et al. (2008) Estimation of standard liver volume for liver transplantation in the Chinese population. *Transplant. Proc.* **40**, 3536–3540, doi:10.1016/j.transproceed.2008.07.135
- 32 van Tellingen, O., Huizing, M.T., Panday, V.R., Schellens, J.H., Nuijten, W.J. and Beijnen, J.H. (1999) Cremophor EL causes (pseudo-) non-linear pharmacokinetics of paclitaxel in patients. *Br. J. Cancer* **81**, 330–335, doi:10.1038/sj.bjc.6690696
- 33 Sparreboom, A., van Zuylen, L., Brouwer, E., Loos, W.J., de Bruijn, P., Gelderblom, H. et al. (1999) Cremophor EL-mediated alteration of paclitaxel distribution in human blood: clinical pharmacokinetic implications. *Cancer Res.* **59**, 1454–1457
- 34 Howgate, E.M., Rowland Yeo, K., Proctor, N.J., Tucker, G.T. and Rostami-Hodjegan, A. (2006) Prediction of in vivo drug clearance from in vitro data. I: impact of inter-individual variability. *Xenobiotica* **36**, 473–497, doi:10.1080/00498250600683197
- 35 Dickinson, G.L., Rezaee, S., Proctor, N.J., Lennard, M.S., Tucker, G.T. and Rostami-Hodjegan, A. (2007) Incorporating in vitro information on drug metabolism into clinical trial simulations to assess the effect of CYP2D6 polymorphism on pharmacokinetics and pharmacodynamics: dextromethorphan as a model application. *J. Clin. Pharmacol.* **47**, 175–186, doi:10.1177/0091270006294279
- 36 Heizmann, P., Eckert, M. and Ziegler, W.H. (1983) Pharmacokinetics and bioavailability of midazolam in man. *Br. J. Clin. Pharmacol.* **16**, 43S–49S
- 37 Ritschel, W.A., Brady, M.E., Tan, H.S., Hoffmann, K.A., Yiu, I.M. and Grummich, K.W. (1977) Pharmacokinetics of coumarin and its 7-hydroxy-metabolites upon intravenous and peroral administration of coumarin in man. *Eur. J. Clin. Pharmacol.* **12**, 457–461
- 38 Wiernik, P.H., Schwartz, E.L., Strauman, J.J., Dutcher, J.P., Lipton, R.B. and Paietta, E. (1987) Phase I clinical and pharmacokinetic study of taxol. *Cancer Res.* **47**, 2486–2493
- 39 Longnecker, S.M., Donehower, R.C., Cates, A.E., Chen, T.L., Brundrett, R.B., Grochow, L.B. et al. (1987) High-performance liquid chromatographic assay for taxol in human plasma and urine and pharmacokinetics in a phase I trial. *Cancer Treat. Rep.* **71**, 53–59
- 40 Brown, T., Havlin, K., Weiss, G., Cagnola, J., Koeller, J., Kuhn, J. et al. (1991) A phase I trial of taxol given by a 6-hour intravenous infusion. *J. Clin. Oncol.* **9**, 1261–1267
- 41 Huizing, M.T., Keung, A.C., Rosing, H., van der Kuy, V., ten Bokkel Huinink, W.W., Mandjes, I.M. et al. (1993) Pharmacokinetics of paclitaxel and metabolites in a randomized comparative study in platinum-pretreated ovarian cancer patients. *J. Clin. Oncol.* **11**, 2127–2135
- 42 Gianni, L., Munzone, E., Capri, G., Fulfaro, F., Tarenzi, E., Villani, F. et al. (1995) Paclitaxel by 3-hour infusion in combination with bolus doxorubicin in women with untreated metastatic breast cancer: high antitumor efficacy and cardiac effects in a dose-finding and sequence-finding study. *J. Clin. Oncol.* **13**, 2688–2699
- 43 Gianni, L., Munzone, E., Capri, G., Villani, F., Spreafico, C., Tarenzi, E. et al. (1995) Paclitaxel in metastatic breast cancer: a trial of two doses by a 3-hour infusion in patients with disease recurrence after prior therapy with anthracyclines. *J. Natl. Cancer Inst.* **87**, 1169–1175
- 44 Duedahl, T.H., Dirks, J., Petersen, K.B., Romsing, J., Larsen, N.E. and Dahl, J.B. (2005) Intravenous dextromethorphan to human volunteers: relationship between pharmacokinetics and anti-hyperalgesic effect. *Pain* **113**, 360–368, doi:10.1016/j.pain.2004.11.015
- 45 Wang, Z., Hall, S.D., Maya, J.F., Li, L., Asghar, A. and Gorski, J.C. (2003) Diabetes mellitus increases the in vivo activity of cytochrome P450 2E1 in humans. *Br. J. Clin. Pharmacol.* **55**, 77–85
- 46 Moller, R.A., Fisher, J.M., Taylor, A.E., Kolluri, S., Gardner, M.J., Obach, R.S. et al. (2006) Effects of steady-state lasofoxifene on CYP2D6- and CYP2E1-mediated metabolism. *Ann. Pharmacother.* **40**, 32–37, doi:10.1345/aph.1G347
- 47 Park, J.Y., Kim, K.A., Park, P.W. and Ha, J.M. (2006) Effect of high-dose aspirin on CYP2E1 activity in healthy subjects measured using chlorzoxazone as a probe. *J. Clin. Pharmacol.* **46**, 109–114, doi:10.1177/0091270005282635
- 48 Liangpunsakul, S., Kolwankar, D., Pinto, A., Gorski, J.C., Hall, S.D. and Chalasani, N. (2005) Activity of CYP2E1 and CYP3A enzymes in adults with moderate alcohol consumption: a comparison with nonalcoholics. *Hepatology* **41**, 1144–1150, doi:10.1002/hep.20673
- 49 Prompila, N., Wittayalerpanya, S. and Komolmit, P. (2007) A study on the pharmacokinetics of chlorzoxazone in healthy Thai volunteers. *J. Med. Assoc. Thai.* **90**, 160–166
- 50 Yang, G., Fu, Z., Chen, X., Yuan, H., Yang, H., Huang, Y. et al. (2011) Effects of the CYP oxidoreductase Ala503Val polymorphism on CYP3A activity in vivo: a randomized, open-label, crossover study in healthy Chinese men. *Clin. Ther.* **33**, 2060–2070, doi:10.1016/j.clinthera.2011.11.004
- 51 Ibrahim, A., Karim, A., Feldman, J. and Kharasch, E. (2002) The influence of parecoxib, a parenteral cyclooxygenase-2 specific inhibitor, on the pharmacokinetics and clinical effects of midazolam. *Anesth. Analg.* **95**, 667–673
- 52 Li, J., Guo, H.-f., Liu, C., Zhong, Z., Liu, L. and Liu, X.-d. (2014) Prediction of drug disposition in diabetic patients by means of a physiologically based pharmacokinetic model. *Clin. Pharmacokinet.* **54**, 179–193, doi:10.1007/s40262-014-0192-8
- 53 Naritomi, Y., Nakamori, F., Furukawa, T. and Tabata, K. (2015) Prediction of hepatic and intestinal glucuronidation using in vitro-in vivo extrapolation. *Drug Metab. Pharmacokinet.* **30**, 21–29, doi:10.1016/j.dmpk.2014.10.001

54 Foti, R.S., Rock, D.A., Wienkers, L.C. and Wahlstrom, J.L. (2010) Selection of alternative CYP3A4 probe substrates for clinical drug interaction studies using in vitro data and in vivo simulation. *Drug Metab. Dispos.* **38**, 981–987, doi:10.1124/dmd.110.032094